https://doi.org/10.1590/jatm.v18.1438 ORIGINAL PAPER

Model to Support Signal Detection Performance of a Laser Proximity Fuze Installed on a Small Air-Defense Missile

Hoang Linh Nguyen[1,*], Hai Tran Van[2]

1. Military Weapon Institute – Hanoi – Vietnam.
2. Le Quy Don Technical University – Faculty of Weapons Technology – Hanoi – Vietnam.

*Corresponding author: nghoanglinh86@gmail.com

ABSTRACT

This paper aims to develop a quantitative model for evaluating the signal detection capability of a laser proximity fuze mounted on small air-defense missiles under strong background noise conditions. The proposed approach integrates three key components: background noise power estimation to characterize environmental effects, signal-to-noise ratio (SNR) computation to relate noise with system parameters, and probability of detection (P_d) evaluation as the primary performance metric. The formulations are established based on quantum photonics and statistical optics, while Monte Carlo simulation is employed to estimate SNR, and the likelihood-ratio test is applied to determine P_d. Numerical results indicate that, among the considered wavelengths (950 nm, 1,300 nm, and 1,550 nm), the 1,550 nm band provides the highest SNR. At a range of 20 m with a transmitted power of 0.01 W, the corresponding P_d reaches 0.76; achieving $P_d = 0.9$ requires increasing the transmitted power to 0.04 W. These findings demonstrate that the proposed model can effectively support the selection of operating wavelength and transmitted power, thereby ensuring reliable signal detection performance of laser proximity fuzes in noisy environments.

Keywords: Laser proximity fuze; Small air-defense missile; Solar background noise; Signal-to-noise ratio; Probability of detection.

INTRODUCTION

Small air-defense missile systems are equipped with laser proximity fuzes to improve target defeat effectiveness. Laser fuzes have many advantages: very high range-measurement resolution, resistance to electro-optical countermeasures (EOCM), compact size, and so on. However, as optical devices, laser fuzes are highly sensitive to environmental effects, such as background noise from solar radiation and backscatter from clouds and fog. Under strong interference, the signal-to-noise ratio (SNR) degrades significantly, reducing the reliability of detecting the return signal from the target. The ability to receive the return signal affects the fuze's overall performance in subsequent operational stages.

The ability to detect the return signal from a target under noisy conditions is evaluated by the probability of detection (P_d). The P_d can be determined experimentally or by probabilistic calculation. The SNR is the ratio between the intensity of the return signal from the target and the intensity of the noise; it depends on the laser source, noise sources, beam propagation processes, and the fuze's technical parameters. Technical parameters that directly affect SNR include laser wavelength, transmitted power (P_T), detector type (positive-intrinsic-negative [PIN] diode or avalanche photodiode [APD]), etc. When designing a fuze, these technical parameters must be chosen to support the ability to detect return signals from targets under complex environmental conditions. Parameter selection must consider the overall relationship among noise sources, fuze technical parameters, SNR, and P_d.

Received: Nov. 12, 2025 | **Accepted:** Mar. 31, 2026
Peer Review History: Single Blind Peer Review.
Section editor: Luiz Martins-Filho

Regarding the performance of laser proximity fuzes in complex environments, in 2006, Chen *et al.* studied four different ranging principles for near-target laser fuzes – geometry intercept, range gating, phase laser proximity, and pseudorandom code – and analyzed the pros and cons of each method. In 2009, Richard D. Richmond compiled the Direct-Detection LADAR System, which uses the likelihood-ratio test (LRT) to compute the P_d (Richmond and Cain 2010). In 2018, Wang *et al.* published a study comparing the detection characteristics of laser fuzes in clouds. Zhou and He (2023) proposed a target recognition method for imaging laser fuzes by combining the Harris and Susan algorithms, aiding the discrimination of target signals from smoke and fog noise. Li and Wang (2014) focused on the design of a low-noise amplifier circuit for APD photodiodes, improving sensitivity for weak returns from small targets. Liu and Chen (2022) used 3-D simulations to evaluate the impact of smoke and dust on the detection capability of multi-channel frequency-modulated continuous-wave (FMCW) laser fuzes and analyzed the influence of component variations on return-signal characteristics and optical countermeasure resilience (Xu *et al.* 2022). More recent research by Guo *et al.* (2024) extends this direction by constructing a 3-D particle collision scattering model for multi-channel laser fuzes to assess anti-noise capability under temporally varying smoke; results show that multi-channel transmit architectures significantly increase detection reliability in complex scattering environments.

Overall, published works have mainly focused on developing signal-processing algorithms and solving individual subproblems for laser fuzes; there is a lack of studies that establish a comprehensive relationship among background noise, SNR, and P_d across different meteorological conditions.

METHODS

This paper simulates the process of receiving and detecting return signals from targets under complex background noise conditions and builds a model to support the signal detection capability of a laser proximity fuze. The model establishes relationships among environmental conditions, the fuze's technical parameters, SNR, and P_d.

RESULTS AND DISCUSSION

The model serves to evaluate the ability to detect return signals under noisy conditions and to recommend technical parameters for the laser fuze, providing a tool to select fuze parameters that support effective signal reception and detection, thereby improving reliability and combat effectiveness in complex environments.

The subproblems are formulated based on quantum photonics and statistical optics, allowing stochastic aspects of optical processes to be taken into account.

The remainder of the paper is structured as follows. First, the proposed model for supporting the signal detection capability of the laser proximity fuze is presented, together with its main components. The influence of background noise is then analyzed, focusing on solar radiation and backscatter from clouds and fog. Next, the signal-to-noise ratio (SNR) is evaluated using a method based on statistical optics combined with Monte Carlo simulation. The probability of detection (Pd) is subsequently determined using the likelihood-ratio test (LRT). The model is then illustrated through a case study on a representative fuze, where the transmitted power is adjusted to meet a required detection probability. The paper concludes with a summary of the main findings and suggestions for future work.

Model to support the signal detection capability of the laser proximity fuze

Product design is a process that combines calculation with the selection of structural and technical parameters. The structural and technical parameters of the product are reasonably selected, suitable for the operational environment, and ensure that the product meets the specified performance requirements. During the signal return acquisition and target detection phase, the laser fuze is strongly affected by background noise sources from the environment. At the same time, it is required to ensure target detection with a high probability, typically with a detection probability of $P_d > 0.9$. The model to support the laser proximity fuze's signal detection capability is a computational tool that recommends the selection of the fuze's technical parameters (Fig. 1). The technical parameters of the fuze include: parameters of the laser transmitter module (such as laser wavelength [λ], P_T, beam

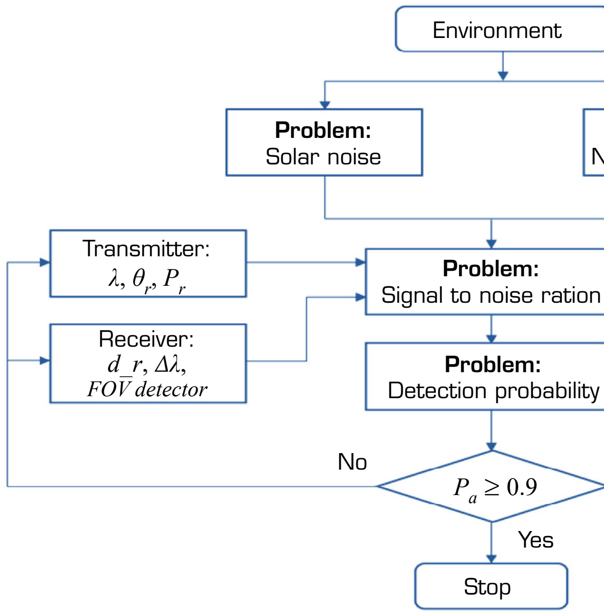

Source: Elaborated by the authors.

Figure 1. Model ensuring the signal detection capability of the fuze.

divergence angle [θ_T], etc.) and parameters of the receiver module (such as receiver aperture diameter [d], optical filter bandwidth [$\Delta\lambda$], and the half field-of-view angle of the receiving optics [FOV]).

The model links three subproblems:

- Calculation of the power of background noise sources entering the receiver;
- Calculation of signal power and the SNR;
- Calculation of the P_d.

The background noise power problem determines the environmental influence on fuze operation. The SNR problem connects the background noise sources with the fuze's technical parameters. The P_d problem is the metric that evaluates whether the fuze can detect the return signal from the target.

These subproblems are formulated using quantum photonics and statistical optics. Signal power and the powers of noise sources are converted into numbers of photoelectrons collected during a laser pulse. The number of photoelectrons due to the signal and due to each noise source is treated as a random variable.

Combining these calculations with the fuze's structural principles produces a tool to select the laser fuze's parameters and support effective signal reception and detection.

Determining the range at which the fuze begins to detect the target

Before performing calculations, the range at which the fuze begins to detect the target must be determined. The fuze detection-start range, R_{laser}, is the distance from the fuze to the point on the target where illumination begins. The detection-start range depends on the relative approach direction between the missile and the target. Figure 2 illustrates the missile approaching the target at different angles.

The detection-start range, R_{laser}, is related to the distance from the detonation point O_{T2} to the target centroid M. One must choose R_{laser} so that the distance from the detonation point to the target centroid, $O_{T2}M$, is less than the lethal radius r_{st}; the limiting case is $O_{T2}M = r_{st}$. R_{laser} must not be excessively large so as to avoid allowing the adversary to detect and employ EOCM. Considering the missile's approach scenarios, when the missile flies parallel to the target ($\eta = 0$), the initial range is the shortest. As the azimuth angle η increases, the fuze's detection-start range R_{laser} also increases. As the largest R_{laser} occurs when the missile's velocity is perpendicular to the target's trajectory (Fig. 2c).

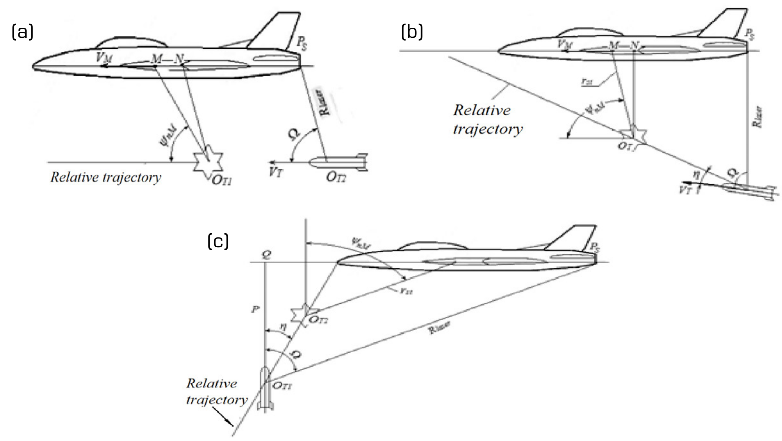

Source: Elaborated by the authors.

Figure 2. Range at which the fuze begins to detect the target. (a) Missile flies parallel to the target; (b) Missile flies obliquely/at an angle towards the target; (c) Missile flies perpendicular to the target.

From the above analysis, this paper selects the maximum detection-start range under the condition that, when the missile velocity V_T is perpendicular to the target velocity, the distance from the detonation point to the target centroid equals the lethal radius (r_{st} = 5.5 m).

For the case where the relative trajectory of the missile is perpendicular to the target trajectory (Fig. 2c), by solving the relevant triangles, one obtains the detection-start radius, R_{laser}, of the fuze:

$$R_{laser} = \frac{r_{st}.\cos(\Psi_{mM}) + V_R \cdot t \cdot \cos(\eta)}{\cos(\Omega)} \quad (1)$$

where t is the fuze's delay time and V_R is the missile's relative velocity.

Operational sequence of the model

The model is operated in the following sequence:

- Set up the configuration and make an initial selection of the fuze's technical parameters; determine the detection-start range, R_{laser}.
- From the fuze's operating environment, compute the power of the background-noise sources.
- Solve the range equations and compute the SNR.
- Compute the P_d and compare it with the required detection threshold.
- Adjust the fuze's technical parameters to support the required detection probability.

Assessment of the impact of background-noise sources

The laser proximity fuze is influenced primarily by two noise sources: solar background radiation and backscattered laser returns from clouds. These two noise sources act under different weather conditions. The assessment of background-noise influence proceeds by analyzing the noise-formation process, calculating the mean noise power within a single pulse, and converting that to the number of photoelectrons.

Solar background noise

Wavelengths used in modern laser proximity fuzes lie in the infrared band and are susceptible to solar background radiation. Solar radiation may enter the receiver optics in the following ways (Fig. 3):

- Sunlight illuminates the target's surface, is reflected back, and enters the receiver.

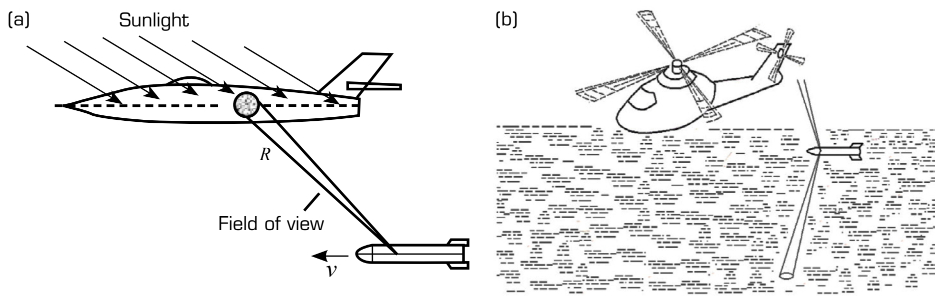

Source: Elaborated by the authors.

Figure 3. Solar radiation incident on the target and the background scene. (a) The sun illuminates the target; (b) The sun illuminates the background.

- Sunlight illuminates the background scene (mountain slopes, ground, water surfaces, etc.), is reflected, and enters the receiver.
- Sunlight shines directly into the receiving aperture.

Sunlight illuminates the target surface with a total solar irradiance S_I = 1,000 W·m². The receiving lens has a diameter $d_r = 2r$ and is located at a range R from the target; the propagating light experiences attenuation characterized by the coefficient T_A. The backscattering from the target surface is distributed uniformly into a solid angle $\theta_R = \pi$. At the entrance of the receiving lens, there is an optical filter; the energy transmission F of the optical filter is determined according to the Stefan-Boltzmann spectral distribution. The power of the background radiation that passes through the optical filter is (Guo *et al.* 2024):

$$P_b = \frac{S_I \cdot \theta_r^2 \cdot \rho \cdot T_A \cdot \pi \cdot r^2}{4} F \quad (2)$$

The flowchart for the algorithm that computes the noise produced by sunlight illuminating the target is shown in Fig. 4. The background noise caused by sunlight illuminating the target has a relatively large value and significantly affects the operation of the fuze. The method of calculating background noise from sunlight illuminating the background scene is similar to the case of sunlight illuminating the target, but with a lower reflectance coefficient.

The power of sunlight entering the receiver lens directly is very large. However, since the field of view (FOV) of the receiving optics is narrow, sunlight can enter the receiver directly only when the solar rays are almost parallel to the optical axis of the receiver lens. This situation rarely occurs.

Backscattered emission noise of the laser beam from clouds

The model for calculating the backscattered noise of the laser beam from clouds and fog is established based on Mie scattering theory. The illuminated region within the cloud or fog has an elliptical shape (Fig. 5).

The reflection coefficient of a water droplet, ρ_N, represents the probability that the scattering angle is $\theta = 180^o$, and it is determined using the Henyey-Greenstein phase function.

According to Mie scattering theory, the particles in the medium are modeled as small spheres with radius r_h and number density N_h. From these parameters, the total backscattering cross-section, Σσ, of the water droplets within a unit volume can be calculated.

Assuming that the backscattered power is uniformly distributed over a hemispherical surface, the power of the backscattered radiation from the cloud or fog that passes through the receiver lens of the fuze is given by:

$$P_{RVC} = P_T \cdot \frac{\Sigma \cdot c \cdot \tau \cdot d_R^2 \cdot e^{-2\alpha R}}{32. R^2} \cdot \eta_A \cdot \eta_B \quad (3)$$

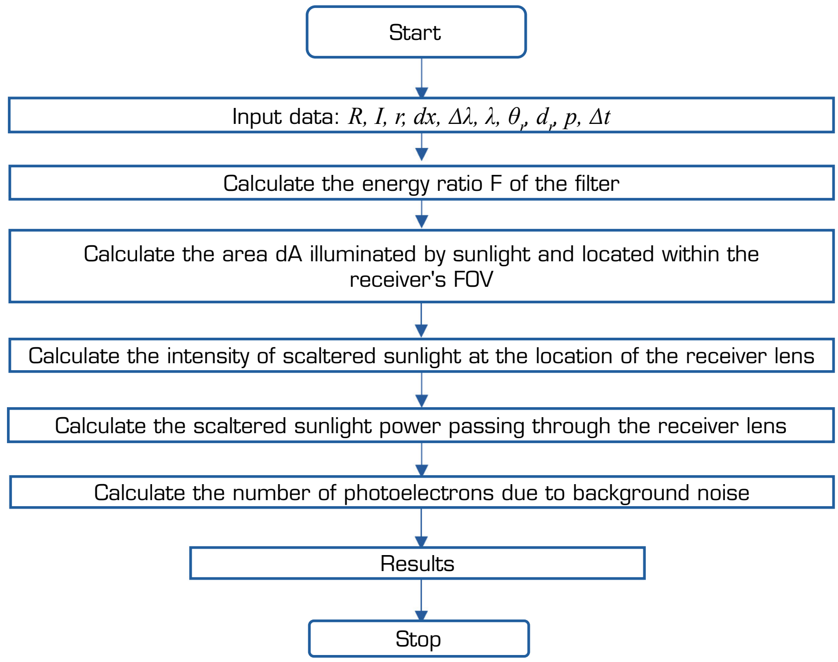

Source: Elaborated by the authors.

Figure 4. Flowchart for determining solar radiation interference noise.

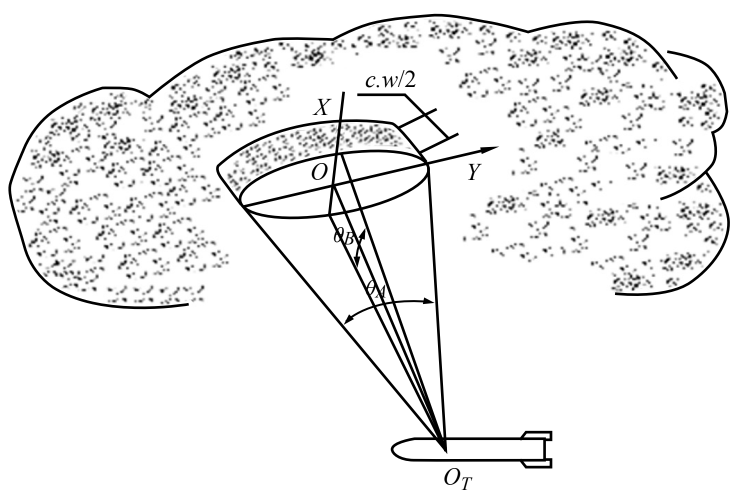

Source: Elaborated by the authors.

Figure 5. Backscatter model from the cloud.

The noise caused by scattering from clouds and fog is directly proportional to the P_T; therefore, its influence cannot be reduced simply by increasing the P_T. The backscattered laser power from clouds and fog, P_{RVC}, is also proportional to the pulse width w. By reducing the pulse width w (for example, $w = 1 \div 2$ ns), the thickness of the illuminated elliptical volume is decreased, thereby reducing the magnitude of the backscattered noise.

Signal-to-noise ratio (SNR)

The formula for calculating the SNR is derived from the range equation, the expressions for background noise, and the formulas for the intrinsic noise components of the receiver unit.

Range equation

The range equation describes the relationship between the P_T and the received signal power P_r. Since the inclination angle of the target surface relative to the transmitted laser beam is unknown, the reflected laser light is assumed to be diffusely scattered uniformly within a solid angle $\theta_R = \pi$.

The range equation is expressed as (Jelalian 1992):

$$P_r = \frac{P_T \cdot \rho \cdot d_r^2 \cdot T_A^2 \cdot \eta_A \cdot \eta_B}{4 \cdot R^2} \tag{4}$$

The received power P_r acts on the photodetector element (photodiode) and is converted into photoelectrons according to the quantum efficiency η. The number of photoelectrons corresponding to the return signal within the collection time interval Δt (Δt = w, with w being the pulse width) is a random variable N_S, whose mean value is:

$$N_s = E[N_S] = \frac{P_r \cdot \eta \cdot w}{h \cdot v} \tag{5}$$

Noise due to random fluctuations in the number of photoelectrons generated by the signal

The number of photons arriving within a collection interval fluctuates randomly, and only a portion of them is converted into photoelectrons. Depending on the target surface characteristics, two types of noise may occur:

Photon counting noise

For a smooth target surface, the number of photoelectrons collected within the time interval Δt follows a Poisson distribution. The fluctuation in the number of photoelectrons gives rise to photon counting noise, which is characterized by the variance of the photon count. For a Poisson-distributed random variable, the variance equals its mean value $E[N_S]$; therefore:

$$\sigma^2 = E[N_S] = \frac{P_r \cdot \eta \cdot \Delta t}{h \cdot v} \tag{6}$$

Speckle noise

When the laser beam illuminates a target surface with significant roughness, the returned signal contains speckle noise. In this case, the number of photoelectrons N_S is a random variable that follows a negative binomial distribution (Richmond and Cain 2010). The speckle noise is characterized by the variance of the photoelectron count N_S, whose value is given by (Richmond and Cain 2010):

$$\sigma_{speckle}^2 = E[N_S]\left(1 + \frac{E[N_S]}{M}\right) \tag{7}$$

where M is the number of degrees of freedom of the light field (also known as the coherence parameter).

Intrinsic noise of the receiver

Dark current

Let the average dark current be $i_{dark} = 0.75 \times 10^{-9}$ A. Electric current represents the amount of charge passing through a cross-section per unit time. The average number of photoelectrons generated by the dark current within the collection interval Δt is given by (Richmond and Cain 2010):

$$E[N_{dark}] = \frac{i_{dark} \cdot \Delta t}{q_e} \tag{8}$$

Both the background noise, N_B, and the dark current noise, N_{dark}, follow Poisson distributions. Because the Poisson distribution is additive, the sum of two Poisson random variables is also Poisson-distributed, with an expected value equal to the sum of their individual expected values.

Thermal noise

Thermal noise arises from the random thermal motion of charge carriers (typically free electrons) within a conductor. Here, thermal noise on the feedback resistor (load resistor) of the amplifier is considered. When converted into photoelectron-equivalent form at the photodetector output, the number of photoelectrons due to thermal noise is denoted as $N_{thermal}$. At temperature T, the variance of the electrical charge caused by thermal noise electrons is given by (Richmond and Cain 2010):

$$Q_n^2 = k_b T\, C / q_e^2 \tag{9}$$

where Q_n is the standard deviation of the number of thermal noise electrons, T is the temperature of the photodetector circuit, C is the capacitance of the circuit, and k_b is Boltzmann's constant.

Calculating the SNR using the Monte Carlo method

Sunlight incident on the target surface is reflected and enters the receiver. A random variable d is defined as the total number of photoelectrons generated by the combined effects of the return signal and all noise sources (collected data):

$$d = N_{speckle} + N_B + N_{dark} + N_{thermal} \tag{10}$$

The SNR in terms of photoelectrons is defined as the ratio of the mean number of photoelectrons generated by the signal to the standard deviation of the total photoelectron count d from all noise sources.

Assuming that all noise components are statistically independent, the standard deviation of the total photoelectron count d can be approximated by the square root of the sum of the variances of the individual noise components.

For a system using a PIN photodiode, the SNR is calculated as:

$$SNR \approx \frac{N_S}{\sqrt{Q_n^2 + \sigma_{thermal}^2 + N_b}} \tag{11}$$

where N_b is the variance (equal to the expected value) of the photoelectron count caused by background noise and dark current.

The paper determines the SNR by statistical estimation using the Monte Carlo method. Multiple simulated range measurements are performed; in each iteration, random values of photoelectron counts are generated for the variables $N_{speckle}$, N_b, N_{dark}, and $N_{thermal}$. After all simulation runs, statistical analysis is carried out to determine the variance of the total random variable d. Using Eqs. 11 or 12, the SNR is then computed.

The algorithm for calculating the SNR is illustrated in Fig. 6.

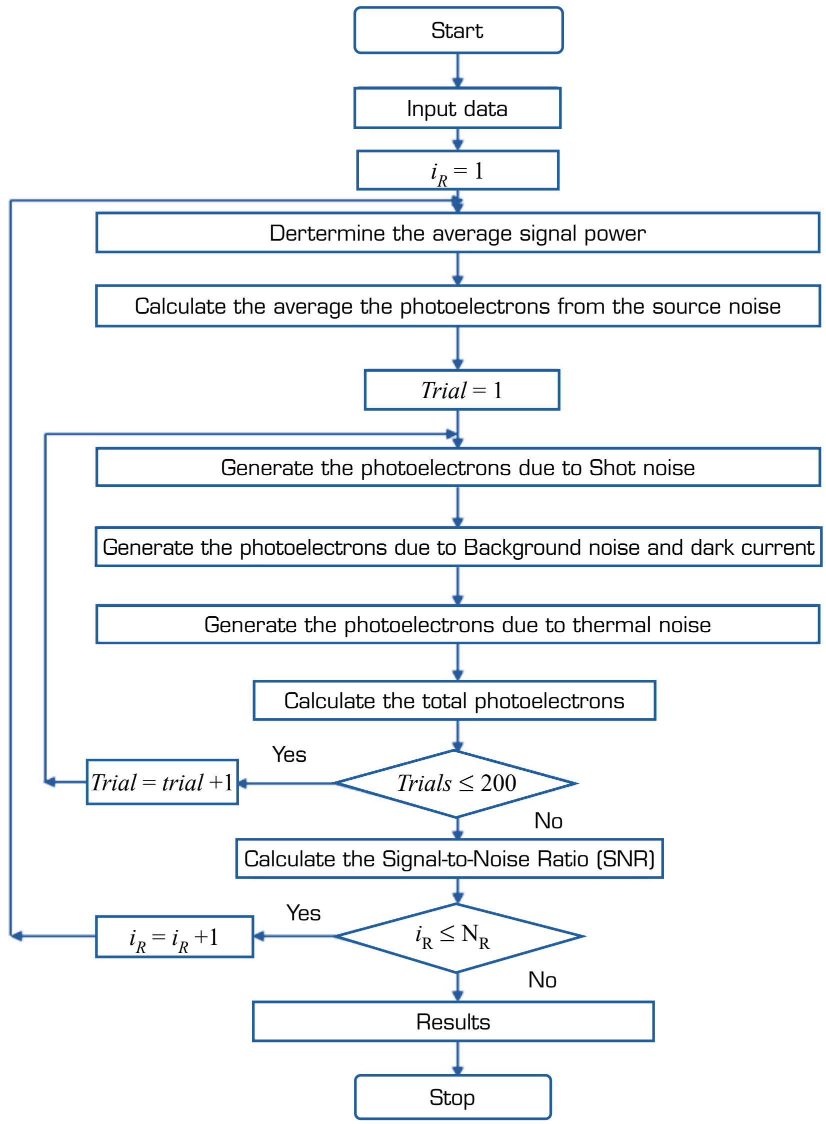

Source: Elaborated by the authors.

Figure 6. Algorithm for calculating SNR.

Target detection probability

The P_d represents the ability of the laser fuze to recognize the return signal from a target under noisy conditions. It serves as an indicator for evaluating the target signal acquisition stage of the fuze. Moreover, P_d is a component parameter contributing to the overall firing effectiveness of the missile system.

This study calculates the detection probability based on the LRT theory. The model uses the probability distributions of both the signal and the noise to determine the detection threshold, while also developing an algorithm to adjust the P_T to support that the required detection probability P_d is achieved.

Expression for detection probability

In a simulated firing, the total number of photoelectrons received, denoted by D, represents the collected data. If the fuze's FOV does not contain a target, the fuze only receives background noise, and the value D tends to be small. If the FOV contains a target, the fuze receives both the target signal and the background noise, so the value D tends to be larger.

In this case, the value D lies within the detection range:

$$D \in D_{target} = (D_{threshold} \div D_{limit}) \tag{12}$$

Establishing two simple statistical hypotheses:

- H_1 – "Target present": the received data d consists of the target signal plus background noise.
- H_0 – "No target": the received data d consists of background noise only.

Let $P(D/H_1)$ with $D \in D_{target}$ denote the partial probability event: "the fuze detects the target when the total number of received photoelectrons takes the given value D." This is a partial event corresponding to each $D \in D_{target}$. The detection probability P_d is then the probability of the event "the fuze detects the target for all possible $D \in D_{target}$," which equals the sum of all mutually exclusive partial probabilities. Mathematically, the total probability of the event "the system can detect the target for all $D \in D_{target}$" is the sum of the component probabilities $P(D/H_1)$ (Jelalian 1992):

$$P_d = \sum_{D \in D_{target}} P(D \mid H_1) \tag{13}$$

Likelihood ratio test (LRT)

Applying the LRT to determine the set D_{target}, the LRT compares the probabilities of two statistical hypotheses: H_1 (Target present) and H_0 (no target). For a single measurement, the total number of received photoelectrons is D. Consider the following probabilities:

- ∈$P(H_1/D)$ – probability that hypothesis H_1 is true; $P(H_0/D)$ – probability that hypothesis H_0 is true.

The LRT selects the hypothesis with the higher probability. It can be stated as:

$$\begin{gathered}\text{If } P(H_1/D) > P(H_0/D) => H_1 \text{ is true;} \\ \text{Otherwise, } => H_0 \text{ is true.}\end{gathered} \tag{14}$$

Using Bayes' conditional probability theorem, and assuming that the number of photoelectrons from the signal follows a negative binomial distribution, and that the number of photoelectrons from background noise (D_B) follows a Poisson distribution, the LRT expression is derived as (Jelalian 1992):

$$\Lambda_l(D) = \frac{-N_B - M \cdot \ln\left(1 + \frac{N_S}{M}\right) - \ln\Gamma(M) + \ln\sum_{D_S=0}^{D} \frac{\Gamma(M + D_S)}{\Gamma(D_S)}\left(1 + \frac{M}{N_S}\right) - D_S \cdot \frac{N_B - D_S}{N_S(D - D_S)!}}{D \cdot \ln(N_B) - N_B - \ln(D!)} \tag{15}$$

For different values of D, the corresponding LRT values are calculated. The set D_{target} includes the values of D for which $LRT < 1$. The value D at which LRT = 1 is considered the threshold that separates the regions target present and no target. The flowchart of the algorithm for computing the detection probability is shown in Fig. 7.

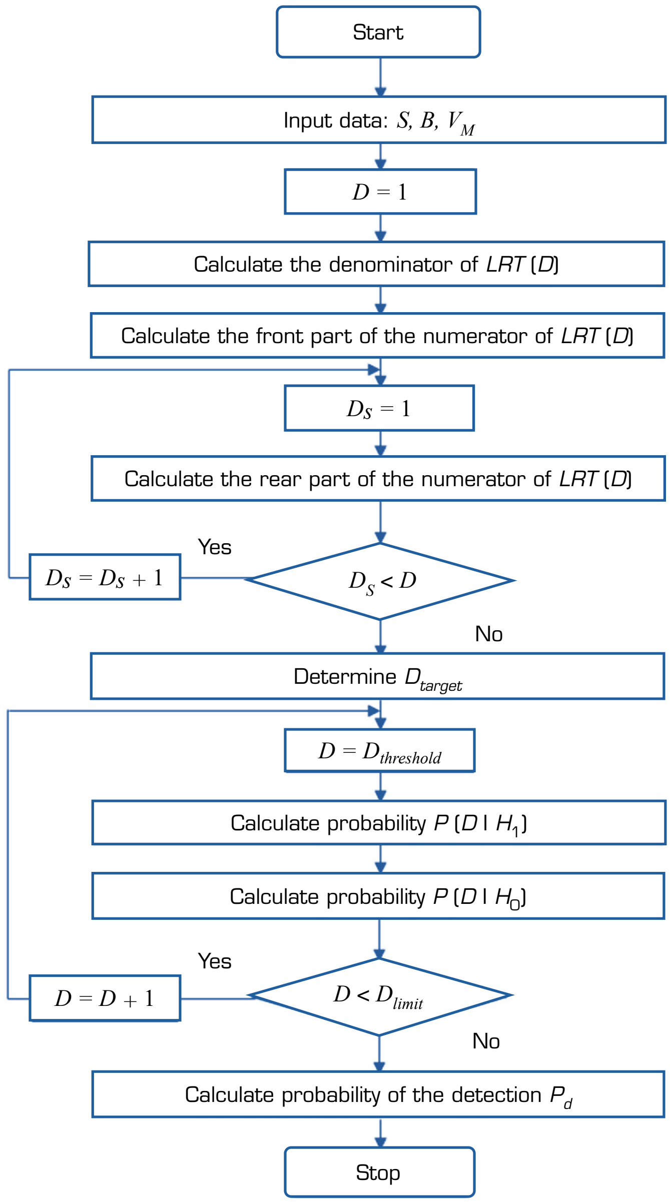

Source: Elaborated by the authors.

Figure 7. Flowchart of the detection probability calculation algorithm.

Case study

Input parameters

Calculation of the target detection range, R_{laser}, for a man-portable air-defense system: pursuit mode, missile velocity V_M = 600 m/s, target velocity is V_T = 400 m/s; the result obtained is R_{laser} = 19.4 m, and the selected detection range is R_{laser} = 20 m.

In combat, if the distance between the point of detonation and the center M of the target is greater than the effective kill radius (r_{st} = 5.5 m), the laser fuze will still detonate, but due to the reduced fragment density, it will only damage the target.

The model is applied to compute results for a fuze with the following parameters: receiver lens diameter d_r = 2 cm; laser wavelength λ = 1,550 nm; optical filter bandwidth Δλ = 56 nm; pulse repetition frequency = 10 kHz; pulse width w = 10 ns.

Calculations are performed for laser wavelengths λ = 900 nm, 1,300 nm, and 1,550 nm, with range varying from R = 1 m to 100 m. The average P_T = 0.01 W.

Assessment of the impact of background-noise sources

Compute the background-noise power due to sunlight illuminating the target surface as a function of range and for the wavelengths 950 nm, 1,300 nm, and 1,550 nm. The results are presented in Table 1.

The variation of background solar noise power with distance and different wavelengths is shown in Fig. 8.

The background noise caused by sunlight reflecting from the target back to the receiver has a relatively high value. At a distance of R = 20 m and wavelength λ = 1,550 nm, the number of noise photons is $N_b = 5{,}234 \times 10^3$, which significantly affects the fuze's operation.

Table 1. Background sunlight noise power (P_b) and number of noise photons (N_b) on the receiver.

R (m)	Wavelengths λ					
	900 nm		1,300 nm		1,550 nm	
0	P_b (W)	N^*_b	P_b (W)	N^*_b	P_b (W)	N^*_b
1	6,1553.10^{-7}	1,3961.10^{4}	2,4612.10^{-7}	8,048.10^{3}	1,4715.10^{-7}	5,738.10^{3}
2	6,1280.10^{-7}	13,875.10^{3}	2,4483.10^{-7}	8,007.10^{3}	1.4644.10^{-7}	5,710.10^{3}
3	6,0902.10^{-7}	13,769.10^{3}	2,435610^{-7}	7,965.10^{3}	1,4573.10^{-7}	5,682.10^{3}
4	6,0522.10^{-7}	13,703.10^{3}	2,4228.10^{-7}	7,924.10^{3}	1,4503.10^{-7}	5,655.10^{3}
5	6,0147.10^{-7}	13,618.10^{3}	2,4101.10^{-7}	7,882.10^{3}	1,4433.10^{-7}	5,628.10^{3}
6	5,9774.10^{-7}	13,534.10^{3}	2,3975.10^{-7}	7,841.10^{3}	1,4363.10^{-7}	5,600.10^{3}
10	5,8049.10^{-6}	13,201.10^{3}	2,3481.10^{-7}	7,678.10^{3}	1,4088.10^{-7}	5,493.10^{3}
20	5,4788.10^{-7}	12,405.10^{3}	2,2280.10^{-7}	7,286.10^{3}	1,3423.10^{-7}	5,234.10^{3}
30	5,1483.10^{-7}	11,656.10^{3}	2,1140.10^{-7}	6,914.10^{3}	1,2790.10^{-7}	4,987.10^{3}
40	4,8377.10^{-7}	10,953.10^{3}	2,0060.10^{-7}	6,560.10^{3}	1,2186.10^{-7}	4,752.10^{3}
50	4,5495.10^{-7}	10,293.10^{3}	1,9034.10^{-7}	6,225.10^{3}	1,1611.10^{-7}	4,528.10^{3}
70	4,0140.10^{-7}	9,088.10^{3}	1,7140.10^{-7}	5,605.10^{3}	1,0541.10^{-7}	4,111.10^{3}
90	3,5444.10^{-7}	8,025.10^{3}	1,5432.10^{-7}	5,047.10^{3}	0,9570.10^{-7}	3,732.10^{3}
100	3,3306.10^{-7}	7,541.10^{3}	1,4643.10^{-7}	4,789.10^{3}	0,9118. 10^{-7}	3.555.10^{3}

Source: Elaborated by the authors.

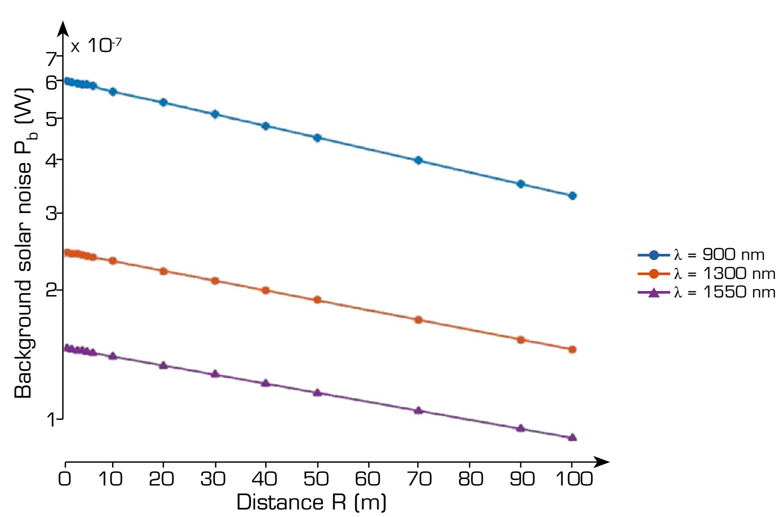

Source: Elaborated by the authors.

Figure 8. Solar background noise power versus distance and wavelength.

The background noise power decreases gradually with increasing distance R; the reduction rate is slow, mainly due to propagation losses. The background noise power entering the receiver depends on wavelength: for longer laser wavelengths, the noise power decreases.

Calculations were performed for two illumination scenarios:

Sunlight reflected from the background scene: assuming sunlight from the zenith is incident directly on a water surface with a reflectance coefficient $\rho_N = 0.1$, the reflected power entering the receiver lens is $N_b = 2.5 \times 10^{-7}$ W.

Direct sunlight entering the receiver: assuming sunlight from the zenith is directly incident on the receiver lens, the solar radiation power entering the receiver is $P_B = 6.58 \times 10^{-3}$ W. The power of direct sunlight entering the receiver is therefore much greater than that of sunlight scattered from the target surface.

Signal-to-noise ratio (SNR)

The proposed model is applied to compute the SNR as a function of distance and wavelength. The results are presented in Table 2.

From the calculation results in Table 2, the SNR decreases as the range increases; the main reason is that the returned signal power from the target decays rapidly (approximately $\propto 1/R^2$), while the background noise power decreases more slowly (mainly due to propagation loss).

Table 2. Results of calculating the SNR with a PIN diode.

R (m)	SNR					
	λ = 900 nm		λ = 1,300 nm		λ = 1,550 nm	
	SNR	SNR(dB)	SNR	SNR(dB)	SNR	SNR(dB)
2	42,295	16,263	61,093	17,860	72,842	18,624
4	10,574	10,242	15,273	11,839	18,210	12,603
6	4,699	6,720	6,788	8,317	8,094	9,081
10	1,692	2,284	2,444	3,881	2,914	4,644
15	0,752	-1,238	1,086	0,359	1,295	1,123
20	0,423	-3,737	0,611	-2,140	0,728	-1,376
30	0,188	-7,259	0,272	-5,662	0,324	-4,898
40	0,106	-9,758	0,153	-8,161	0,182	-7,397
50	0,068	-11,696	0,098	-10,099	0,117	-9,335
70	0,035	-14,618	0,050	-13,021	0,059	-12,258
90	0,021	-16,801	0,030	-15,204	0,036	-14,440
100	0,017	-17,716	0,024	-16,119	0,029	-15,356

Source: Elaborated by the authors.

The wavelength 1,550 nm gives the highest SNR at all ranges among the three studied wavelengths, primarily because of better atmospheric transmission, especially in the presence of clouds.

The variation of the SNR with distance R at the wavelength 1,550 nm is shown in Fig. 9.

Calculation of P_d and adjustment of P_T

For a receiver using a PIN diode, at $R = 20$ m and average transmit power $P_T = 0.01$ W, with laser wavelength 1,550 nm:

- The number of photoelectrons produced by the return signal is $N_S = 34.10^2$.
- The background noise produces $N_B = 46 \times 10^2$ photoelectrons.

At close ranges, the number of signal photoelectrons, N_S, is very large. To reduce computational load, photoelectrons can be grouped into packets; each packet contains 102 photoelectrons.

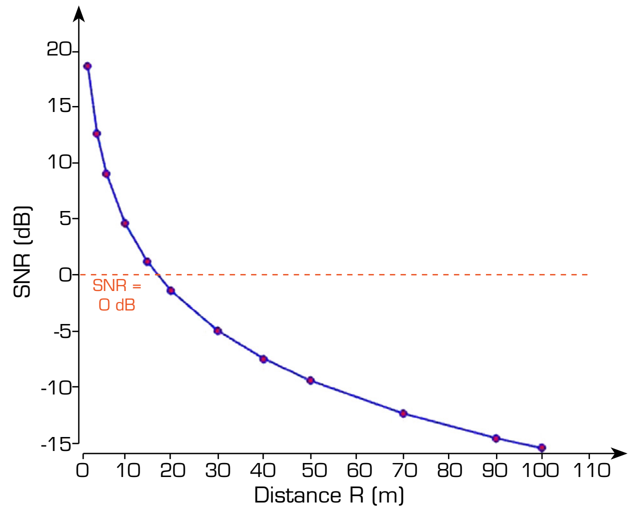

Source: Elaborated by the authors.

Figure 9. Variation of SNR versus distance at wavelength 1,550 nm.

Compute the LRT(D) values for D over the range ($1/D_{limit}$); use the LRT(D) curve to determine the detection threshold. In Fig. 10, the LRT(D) curve intersects the line LRT(D) = 1 at the threshold value $D_{threshold} = 57 \times 10^2$. Values below this threshold correspond to the target-present region (Fig.10).

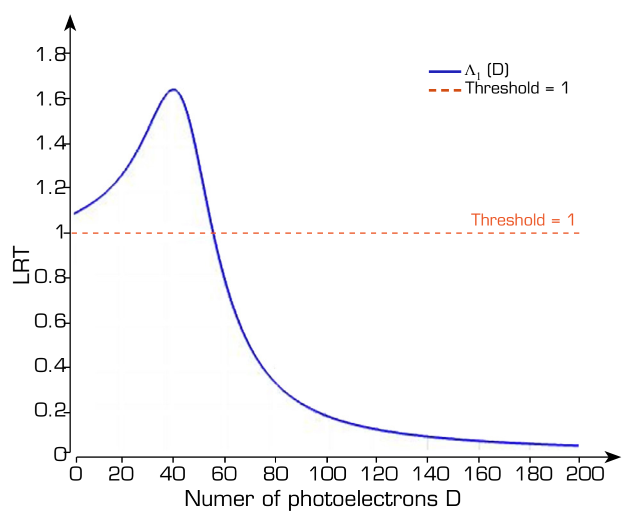

Source: Elaborated by the authors.

Figure 10. LRT as a function of the total number of photoelectrons D.

Adjusting P_T to achieve the required detection probability

Calculating the detection probability P_d to verify that the fuze can complete the signal-acquisition and detection stage for target returns. In design, one must also solve the inverse problem: adjust the P_T so that the detection probability meets the required level.

At a considered range R, use Eq. 4 to determine the mean number of photoelectrons from solar background noise N_b = B. Initially, choose an average P_T; solve the range equation to obtain the received signal power P_r, which corresponds to a mean number of signal photoelectrons $N_S = S_1$. Compute the detection probability P_d. If P_d is not sufficiently large, adjust the P_T to increase the number of returned photoelectrons N_S until the detection probability reaches the required value (typically $P_d \geq 0.9$).

For the laser fuze with average $P_T = 0.01$ W, at range R = 20 m, the mean number of photoelectrons from background noise is $N_b = 46 \times 10^2$. Compute the detection probability while varying the signal photoelectron count N_S from $S_1 = 34.10^2$ up to $S_{max} = 200.10^2$, and plot P_d (S). From this plot, determine the value of N_S that yields the required detection probability.

The curve P_d (S) is shown in Fig. 11. With $N_S = 34 \times 10^2$ signal photoelectrons, the detection probability is $P_d = 0.76$. Therefore, the P_T must be increased to meet the required detection probability (according to the fuze standard IL-STD-1316, a typical requirement is $P_d \geq 90\%$).

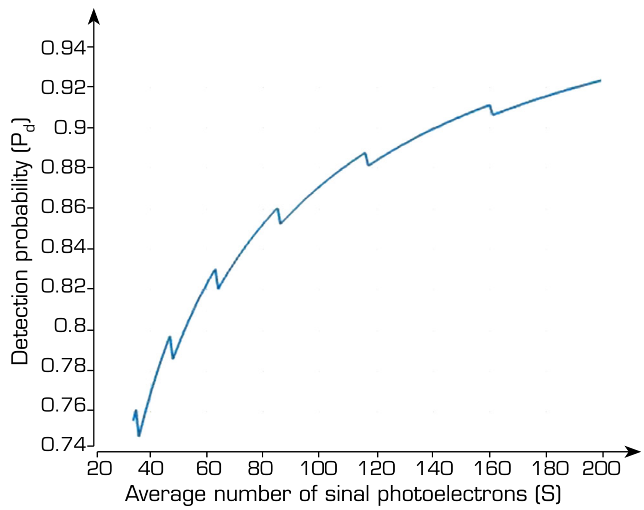

Source: Elaborated by the authors.

Figure 11. Number of photoelectrons corresponding to the detection probability.

The $P_d(S)$ curve exhibits a sawtooth-like shape, as the set of valid detection counts D does not vary continuously but changes in discrete steps according to the detection threshold $D_{threshold}$. The threshold-crossing condition is satisfied only at specific discrete values, causing D to change stepwise as the signal level S varies. Consequently, the detection probability jumps between successive levels, leading to the observed drops and the characteristic sawtooth pattern in the curve.

From the required number of photoelectrons, the P_T can be calculated inversely. Figure 10 shows that the desired detection probability is achieved when $N_S \approx 141 \times 10^2$ photoelectrons. To support $P_d = 0.9$, the corresponding required average is $P_T = 0.04$ W.

Relationship between average P_T, P_d, and SNR

Using different values of average P_T, the range Eq. 4 is used to compute the received power P_r and the corresponding mean number of collected photoelectrons N_S. Equation 12 is then used to compute the SNR and the detection probability P_d at range $R = 20$ m. The results are presented in Table 3.

The results of the SNR and the detection probability P_d for different values of average P_T are shown in Fig. 12.

As the average P_T increases, the SNR also increases, which in turn raises the detection probability P_d. When $P_T < 0.005$ W, SNR < 1, and the signal is buried in noise. Starting from $P_T \approx 0.02$ W, with SNR ≈ 1.5-2, the system begins to detect the target signal.

At the threshold $P_T \approx 0.04$ W-0.05 W, SNR ≈ 3-4, and the detection probability is $P_d \approx 0.75$; the system reliably detects the target signal. To achieve $P_d \geq 0.9$ requires $P_T \geq 0.04$ W, corresponding to SNR ≈ 6 *dB*.

CONCLUSION

This paper studies the initial operational stage of a laser proximity fuze and has developed a model to support the signal detection capability applied to small air-defense missiles. Using quantum photonics and statistical optics, the model formulates three basic

Table 3. Signal-to-noise ratio versus P_d.

Pavg (*W*)	*NS*	SNR	SNR (*dB*)	P_d
0.001	3.35	0.07	-11.38	0.52
0.002	6.70	0.15	-8.37	0.55
0.003	10.05	0.22	-6.61	0.60
0.004	13.40	0.29	-5.36	0.63
0.005	16.75	0.36	-4.39	0.65
0.006	20.10	0.44	-3.59	0.66
0.007	23.45	0.51	-2.93	0.70
0.008	26.80	0.58	-2.35	0.71
0.009	30.15	0.66	-1.83	0.73
0.01	33.50	0.73	-1.38	0.75
0.02	67.01	1.46	1.63	0.83
0.03	100.52	2.19	3.39	0.87
0.04	134.03	2.91	4.64	0.90
0.05	167.54	3.64	5.61	0.91
0.06	201.04	4.37	6.41	0.92
0.07	234.55	5.10	7.07	0.93
0.08	268.06	5.83	7.65	0.94
0.09	301.56	6.56	8.17	0.94
0.1	335.07	7.28	8.62	0.94

Source: Elaborated by the authors.

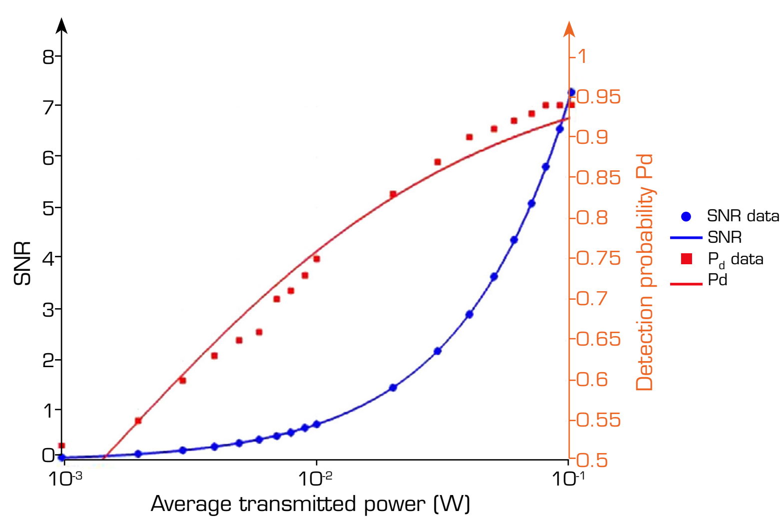

Source: Elaborated by the authors.

Figure 12. Relationship between the SNR and the detection probability P_d for different values of average P_T.

problems for the fuze's signal-acquisition and detection stage. By analyzing the mechanisms that produce typical background noise for optical fuzes, the paper derives expressions to compute noise power from solar irradiation and from backscattering in clouds. The SNR is calculated in photoelectron units by Monte Carlo simulation. The detection probability P_d is determined via the LRT. The use of statistical optics allows the model to account for the randomness of optical processes. The subproblems were implemented as computational modules simulating the signal acquisition stage of the fuze. The proposed model is an effective tool for the design of laser fuzes. The calculation results support the selection of structural and technical parameters such as laser wavelength, P_T, and photodetector type. The model was applied to a specific fuze and used to recommend adjustments to P_T to meet detection requirements.

The model provides a scientific basis and a useful engineering tool for designing laser fuzes or evaluating specific fuze prototypes. From the model for the receiving and detection stage, further extensions to the subsequent signal-processing stage are possible. Connecting the three subproblems studied here with range-estimation and detonation-command problems would describe the fuze's full operation. If linked with reliability-assessment problems (probability of failure) and evaluation of fragment lethality, the result would be an integrated model for assessing the overall "combat effectiveness of the warhead."

CONFLICT OF INTEREST

Nothing to declare.

AUTHOR CONTRIBUTIONS

Conceptualization: Nguyen HL; **Methodology:** Nguyen HL; **Writing - Original Draft:** Nguyen HL; **Writing - Review & Editing:** Nguyen HL and Van HT; **Final approval:** Nguyen HL.

DATA AVAILABILITY STATEMENT

All data sets were generated or analyzed in the current study.

FUNDING

Not applicable.

DECLARATION OF USE OF ARTIFICIAL INTELLIGENCE TOOLS

AI tools (e.g., ChatGPT) were used for language editing only. All scientific content was developed and verified by the authors.

ACKNOWLEDGEMENTS

Not applicable.

REFERENCES

Chen HM, Zhang Q, Liu Y (2006) Laser fuze detection techniques using different methods. Opt Precis Eng 14(5):789-795. https://doi.org/10.1080/03052150600746931

Guo Z, Yang B, Wu K, Liang Y, Hao S, Huang Z (2024) FMCW laser fuze structure with multi-channel beam based on 3D particle collision scattering model under smoke interference. Sensors 24(16):5395. https://doi.org/10.3390/s24165395

Jelalian A (1992) Laser radar systems. Norwood: Artech House.

Li J, Wang D (2014) Design of low noise receiving amplifier circuit for laser proximity fuze. J Electron Meas Instrum 28(2):112-118.

Liu R, Chen Y (2022) Virtual simulation of the effect of FMCW laser fuse detector's component performance variability on target echo characteristics under smoke interference. Chin J Lasers 49(12):128-136. https://doi.org/10.3390/ma15124268

Richmond RD, Cain SC (2010) Direct-detection LADAR systems (SPIE Tutorial Texts in Optical Engineering, Vol TT85). Bellingham: SPIE Press. https://doi.org/10.1117/3.836466

Wang F, Chen H, Yang S, Xu L (2018) Comparison of detection performance of near-, mid-, and far-infrared laser fuzes in clouds. Appl Opt 57(27):8018-8025. https://doi.org/10.1364/AO.57.008078

Xu T, Zhao K, Sun L (2022) FMCW laser fuze structure with multi-channel beam based on 3D particle collision scattering model under smoke interference. Infrared Laser Eng 51(6):135-142. https://doi.org/10.3390/s24165395

Zhou Y, He W (2023) Target recognition method of laser imaging fuze. J Appl Optoelectron 45(3):215-223. https://doi.org/10.7510/jgjs.issn.1001-3806.2023.02.017